Geophys. J. Int. (2007) **171,** 339–351 doi: 10.1111/j.1365-246X.2007.03519.x

Seismic anisotropy beneath Dronning Maud Land, Antarctica, revealed by shear wave splitting

Bettina Bayer,[1] Christian Müller,[2] David W. Eaton[3] and Wilfried Jokat[1]

[1]*Alfred-Wegener-Institut für Polar- und Meeresforschung, Am alten Hafen* 26, D-27568 *Bremerhaven, Germany. E-mail: bbyer@awi-bremerhaven.de*
[2]*FIELAX GmbH, Bremerhaven, Germany*
[3]*Department of Earth Sciences, University of Western Ontario, London, ON* N6A 5B7, *Canada*

Accepted 2007 June 7. Received 2007 June 7; in original form 2007 March 20

SUMMARY

Shear wave splitting analyses have been carried out using teleseismic data from broad-band seismograph stations deployed at temporary and permanent locations in Dronning Maud Land (DML), Antarctica. In most cases, the observed anisotropy can be related to major tectonic events that formed the present-day Antarctic continent. We rule out an anisotropic contribution from recent asthenospheric flow. At the Russian base Novolazarevskaya near the coast in central DML, waveform inversion suggests a two-layer model where the fast direction of the upper layer is oriented parallel to Archean fabrics in the lithosphere, whereas the anisotropy of the lower layer is interpreted to have been created during the Jurassic Gondwana break-up. Recordings at the South African base Sanae IV, however, show enigmatic results. For narrow backazimuthal segments, splitting parameters show strong variations together with a multitude of isotropic measurements, indicative of complex scattering that cannot be explained by simple one- or two-layer anisotropic models. In the interior of the continent, the data are consistent with single-layer anisotropy, but show significant spatial variations in splitting parameters. A set of temporary stations across the Heimefront shear zone in western DML yield splitting directions that we interpret as frozen anisotropy from Proterozoic assembly of the craton. An abrupt change in fast axis direction appears to mark a suture between the Grunehogna craton, a fragment of the Kalahari–Kaapvaal craton in southern Africa and the Mesoproterozoic Maudheim Province.

Key words: anisotropy, Antarctica, fossil deformation, Precambrian suture, shear wave splitting.

1 INTRODUCTION

The present-day Antarctic continent constitutes a key geological record of several major tectonic and thermal events during Earth's history. During the existence of both Rodinia and Gondwana, for example, Antarctica occupied a central part of a united landmass. Although 98 per cent of the continent is covered with ice, tracks of collisions and orogenies, spreading, rifting, strike-slip deformation as well as subsequent continental break-up have been documented.

The present study focuses on Dronning Maud Land (DML) (Fig. 1), a region of Antarctica composed of a collage of crustal blocks ranging in age from Archean to early Palaeozoic. Regional models from surface wave tomography show that DML is underlain by a typical Precambrian cratonic lithosphere with a thickness of ∼220 km (Morelli & Danesi 2004), consistent with the ∼210 km thermal lithospheric thickness characteristic of Archean cratons in the southern hemisphere (Artemieva & Mooney 2001).

Through the investigation of shear wave birefringence (splitting) it is possible to obtain information about strain fabrics and tectonic deformation processes that characterize cratonic lithosphere (Silver 1996; Savage 1999; Eaton & Jones 2006). In the upper mantle, seismic anisotropy arises primarily from strain-induced lattice-preferred orientation (LPO) of the dominant mineral, olivine (Montagner 1994). Anisotropy is mainly located in the litosphere in regions with low tectonic activity. Strain fabrics associated with fossil lithospheric anisotropy, recent mantle flow, aligned cracks, crustal melt filled pockets or combinations thereof have been invoked to explain observed splitting patterns (Savage 1999).

Often it is possible to distinguish different source (crust, mantle, fracture or else) of anisotropy by using different kind (frequency) of data, as teleseism or local seismicity. Sometime, the lack of some type of seismicity makes it necessary to have other information to be added to anisotropy pattern. Additional knowledge about, for example, magnetic or gravity anomalies of the investigated area may be very helpful features to identify the source of anisotropy.

In particular, two commonly cited causes of upper mantle anisotropy are vertically coherent deformation (VCD) of the lithosphere that formed during orogenic assembly of the craton (Silver 1996) and viscous drag at the base of the lithosphere arising from absolute plate motion (APM) (Vinnik *et al.* 1992).

Here, we present new shear wave splitting observations from 10 broad-band seismograph stations in central DML. Our attention

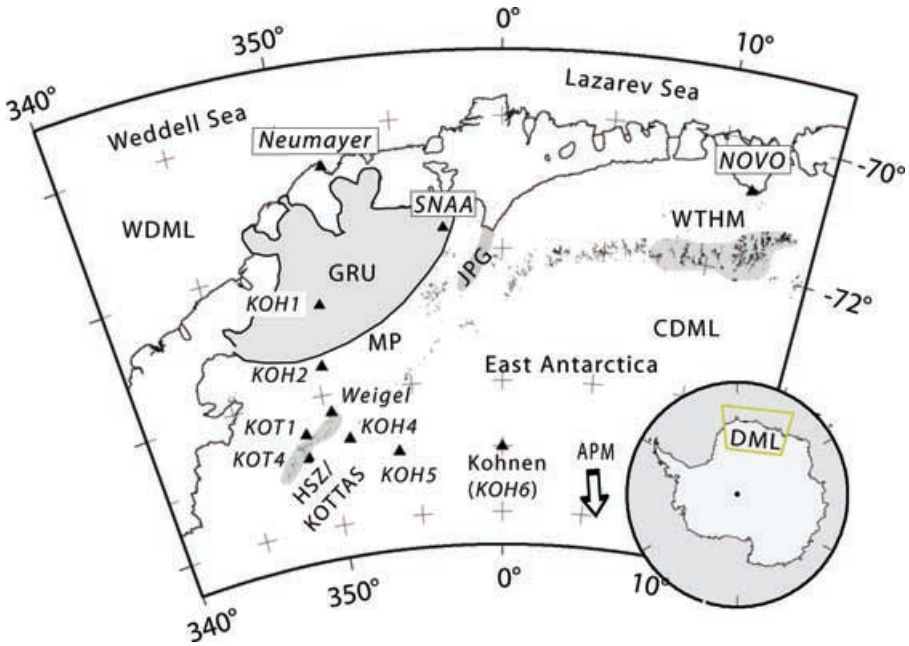

Figure 1. Sketch of Dronning Maud Land. Main geological units mentioned in the text are grey shaded. Abbreviations are: HSZ, Heimefront shear zone; KOTTAS, Kottas mountains; JPG, Jutul-Penck-Graben covered by the Jutulstraumen glacier; GRU, Grunehogna craton; WTHM, Wohlthat massif; MP, Maudheim province; KOH, stations deployed across the HSZ; KOT, stations deployed within KOTTAS; Weigel, station deployed on Weigel nunatak (an outcrop at KOTTAS); NOVO, Russian station Novolazarevskaya; SNAA, South African station Sanae IV; CDML, Central Dronning Maud Land; WDML, Western Dronning Maud Land; APM, Absolute Plate Motion given by Gripp & Gordon (1990) with an asthenospheric flow direction of 170° and a plate velocity of 1.15 cm a^{-1}; Outcrops are marked with black dots.

focuses on the relationship between anisotropic structures within the lithosphere and tectonic deformation processes. Our observations are sparse, out of logistical necessity due to the harsh conditions in Antarctica; nevertheless our results provide significant new constraints on tectonic architecture and the nature of processes involved in the lithospheric assembly of the continent.

2 GEOLOGICAL AND TECTONIC SETTINGS

Several major geological and tectonic events during Earth's history formed the present-day Antarctic continent. Within the area of investigation (DML), the most prominent tectonic fabrics were formed during several phases: The Grenville event, *ca*. 1.1 Ga, which formed the supercontinent Rodinia; the Ross-/Pan-African event at 500 Ma, forming the supercontinent Gondwana due to the collision between West and East Gondwana; the break-up of Gondwana 160 Ma ago, which started in the Lazarev Sea (the ocean basin off DML) accompanied by voluminous volcanism, magmatism, and major outpourings of continental flood basalts (e.g. Jacobs *et al.* 2003).

In western DML, an Archean cratonic fragment named Grunehogna craton (GRU) is exposed (Fig. 1). It consists of Archean granitic gneisses and Mesoproterozoic sedimentary rocks of similar ages to the Kalahari–Kaapvaal craton in southern Africa. GRU is most likely a piece of the Kalahari–Kaapvaal craton dispersed during fragmentation of Gondwana (Groenewald *et al.* 1991). The entire southern side of GRU is rimmed by the Maudheim province (MP) comprised of Proterozoic high-grade metamorphic rocks of Grenvillian age (1.2–1.0 Ga). This MP is likely continued as the Namaqua-Natal belt in southern Africa.

The western margin of the East African Orogen, named East Antarctic Orogen, is exposed in Heimefrontfjaella with the Grenvillian-age Heimefront shear zone (HSZ) as its western front. The HSZ juxtaposes crust to the east, characterized by a pervasive Pan-African overprint, against crust to the west where tectonothermal effects of the Pan-African event are weak to non-existent. Central DML most likely represents the southern continuation of the Mozambique belt into East Antarctica. In this region, Jacobs *et al.* (2003) reported evidence for asthenospheric upwelling, followed by mantle delamination of the orogenic root, surface uplift and subsequent orogenic collapse.

The passive volcanic continental margins off WDML and CDML, formed during the Gondwana break-up, border the Weddell Sea and the Lazarev Sea, respectively. Following Cox (1992), the initial part of the break-up can be described by a two-stage model. In the first stage, about 200-190 Ma, pre-existing Permo-Triassic shear zones were reactivated, causing Africa and Antarctica to move apart as a result of strike-slip movement accompanied by a massive outflow of mantle-derived magmas. In the second stage, about 170 Ma, seafloor spreading commenced and the two continents drifted away from each other.

3 DATA AND METHOD

During several experiments, portable broad-band seismometers (Lennartz 20 s/5 s) with RefTek recording systems were deployed various parts of DML (Fig. 1 and Table 1). These experiments were carried out across the HSZ during the south polar summer of 2003 and along the Kottas mountain range during the south polar summer of 2004, both in western DML (Fig. 1). The duration of recordings varied and depended strongly on weather conditions and technical robustness of the equipment. In most cases, less than 5 weeks of data were recorded. Nevertheless, a sufficient number of core shear waves were observed (Fig. 2) to enable robust shear wave splitting results to be obtained.

Table 1. Splitting parameters for stations deployed across the Heimefront shear zone (KOH1–KOH6), within Kottas mountains (KOT1-KOT4, Weigel), South African base Sanae IV (SNAA), and Russian base Novolazarevskaya (NOVO). Column 'Phases' denotes the total number of included phases, column 'Good' denotes clear observable anisotropy of included phases; difference between them represents nulls. If more than one phase was included the stacking method of Wolfe & Silver (1998) was applied that is denoted by the abbreviation WS. Shortcut for a single measurement is SC after (Silver & Chan 1991). 2L is denoted to a two-layer solution found for NOVO and for the permanent stations VNA2 and VNA3 (Müller 2001).

Station	Latitude (°)	Longitude (°)	Fast axis θ (°)	Time delay δt (s)	Phases	Good	Method
KOH1	−09.310	−72.648	67 ± 6	0.90 ± 0.25	8	4	WS
KOH2	−09.713	−73.563	77 ± 6	0.90 ± 0.16	6	4	WS
KOH4	−08.794	−74.713	63 ± 6	1.05 ± 0.26	6	4	WS
KOH5	−06.055	−75.004	3 ± 1	1.20 ± 0.00	5	3	WS
KOH6 (Kohnen)	00.075	−75.002	73 ± 5	–	5	–	WS
Weigel	−09.622	−74.275	86 ± 5	0.94 ± 0.25	13	7	WS
KOT1	−11.337	−74.908	34 ± 4	1.69 ± 0.13	1	1	SC
KOT4	−11.258	−74.553	27 ± 7	1.50 ± 0.27	1	1	SC
SNAA	−02.838	−71.671	–	–	101	25	SC
NOVO	11.835	−70.776			23		2L
VNA2	−7.392	−70.926			–		2L
VNA3	−9.670	−71.243			–		2L

Temporary deployed stations across HSZ (KOH1–KOH6) were sited on ice that increases in thickness towards south, reaching a maximum thickness of 3 km underneath summer drilling station Kohnen (KOH6). Stations along the Kottas mountain range (Weigel, KOT1, KOT4) were deployed directly on exposed rocks (Fig. 1). In addition, permanent broad-band recordings from 2002 to 2005 at the South African base SANAE IV (SNAA) were investigated and yielded the greatest number of observations. We also used recordings of seismographs, operated during the south polar winter 2005 at the Russian base Novolazarevskaya (NOVO) in central DML and at Weigel nunatak in the Kottas mountains.

For each seismograph, all events with magnitude greater than 5.5 and epicentral distance greater than 85° were visually inspected. A bandpass filters with corners at 0.03 and 0.5 Hz was applied to improve the signal-to-noise ratio (SNR). We then computed splitting parameters (fast polarization direction, θ, and time delay, δt) using the method of Silver & Chan (1991). For a single event, this method performs and exhaustive search of splitting parameter to find the pair that best reverses the splitting process within a selected time window. Two criteria may be used, either minimizing the energy of the transverse component or minimizing the smaller eigenvalue of the covariance matrix. Both methods were applied and compared for core shear waves SK(K)S, but only the second method was used in the case of S(cS) phases generated by deep teleseismic earthquakes.

Following established practice for shear wave splitting analysis, we classified our measurements according to five criteria. A measurement defined as good quality satisfies the following: A distinct phase arrival is visible on the radial and transverse components, with a SNR of 2 or greater; prior to the splitting correction, the particle motion in the horizontal plane is elliptical; after the splitting correction, the particle motion is linear; the shape of the recovered fast and slow split shear waves are very similar; and the contour representing the 95 per cent confidence interval contains a well defined closed region in the energy diagram (Fig. 3). Measurements defined as fair quality fulfil these five criteria but without such a high degree of confidence.

So-called null measurements are characterized by weak or absent transverse signals, and consequently particle motion that is roughly linear. For such events, the energy contour plot is elongate, which means that no unique splitting parameter pair is found that adequately minimizes the transverse energy and/or smaller eigenvalue (Fig. 4). Null measurements may be due to absence of anisotropy (isotropic conditions), vertical anisotropy with an *a*-axis of the olivine crystal aligned in the direction of shear wave propagation, or incoming wave polarization along the fast or slow azimuth of the fast axis. When nulls are measured at a wide variety of azimuths for shear waves with steep incident angle, a common interpretaton is that the medium is either effectively isotropic or transversely isotropic with a vertical symmetry axis (Savage *et al.* 1996).

To obtain the best-fitting splitting parameters for all phases recorded at a single station and to ensure a relatively equal weight for all measurements, we applied the stacking method of Wolfe & Silver (1998), originally devised to study anisotropy at noisy oceanic stations. This method enables the analysis of events considered to have fair quality, which might otherwise be discarded. We remark that the stacking method assumes that the splitting observations do not exhibit backazimuthal variations, as expected for a single homogeneous anisotropic layer with a vertical symmetry axis. An example for the stacking method for station KOH4 is given in Fig. 5.

At some stations we observed significant variations in the apparent splitting parameters as a function of incoming shear wave polarization (or simply the backazimuth in the case of shear waves traversing through the outer core). One possible explanation for this behaviour is the presence of two or more anisotropic layers. In the simple case of a double-layered anisotropic medium, apparent splitting parameters are expected to show a characteristic $\pi/2$-periodicity (Silver & Savage 1994). This $\pi/2$-pattern is considered diagnostic of two-layer anisotropy, and can help to distinguish this scenario from other conditions such as single-layer with dipping symmetry axis or anisotropy caused by a inhomogenous medium (Fouch & Rondenay 2006).

We have also applied the waveform inversion method of Özalaybey & Savage (1994) to our best quality split waveforms. This method is a generalization of the single-layer stacking method of Wolfe & Silver (1998). It searches for the four parameters for a double-layer anisotropic model using the radial and transverse waveforms directly, rather than the indirect approach of fitting apparent single-layer splitting parameters versus backazimuth. The waveform inversion approach has several advantages over the latter method. First, it does not require as large a range backazimuths, since waveforms contain more information than the apparent

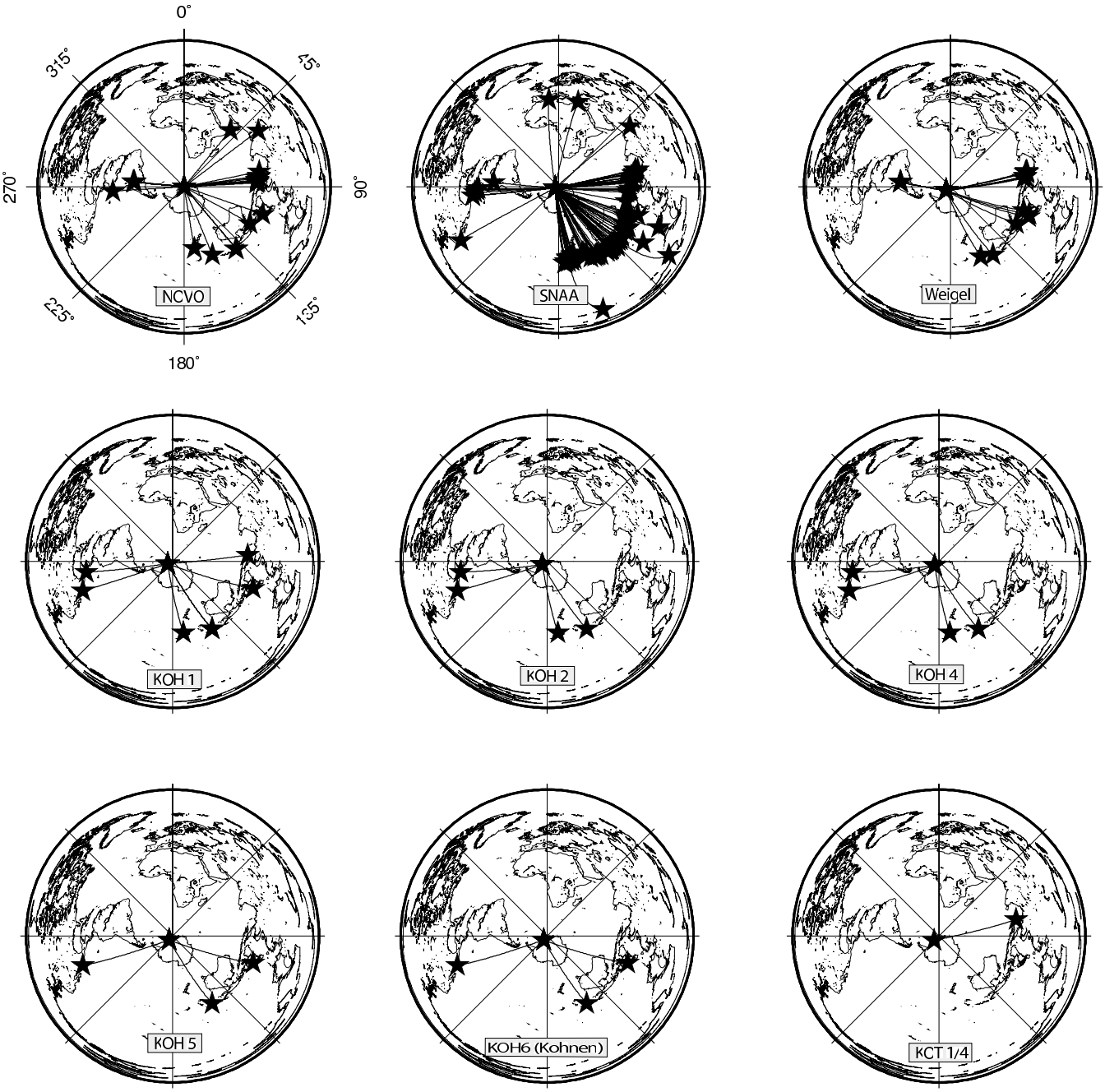

Figure 2. Distribution of teleseismic events expressed as black stars used in this study. They are plotted in an azimuthal equidistant projection with the station location (grey star) in the centre.

splitting parameters. Second, the waveform inversion method yields formal estimates of parameter uncertainty via the *F*-test (Eaton *et al.* 2004), useful for evaluating the statistical significance of the inferred layer parameters.

4 RESULTS

In general, the results we retrieved are sufficiently different from each other that no single model is valid for all stations (Fig. 6). Therefore, this section (as well as the section covering interpretation and discussion) will be separately presented in three subsections: first for temporary deployed stations within WDML and across the HSZ, second for coastal station NOVO in CDML and third for station SNAA.

A complete overview about the single splitting parameters for all events used in the present study is provided as online supplementary data.

4.1 Results for Heimefront shear zone, WDML

For all inland stations of western DML, no evidence were found for a two-layer medium by applying the waveform inversion technique of Özalaybey & Savage (1994). The individual results retrieved from these technique are listed in Table 2.

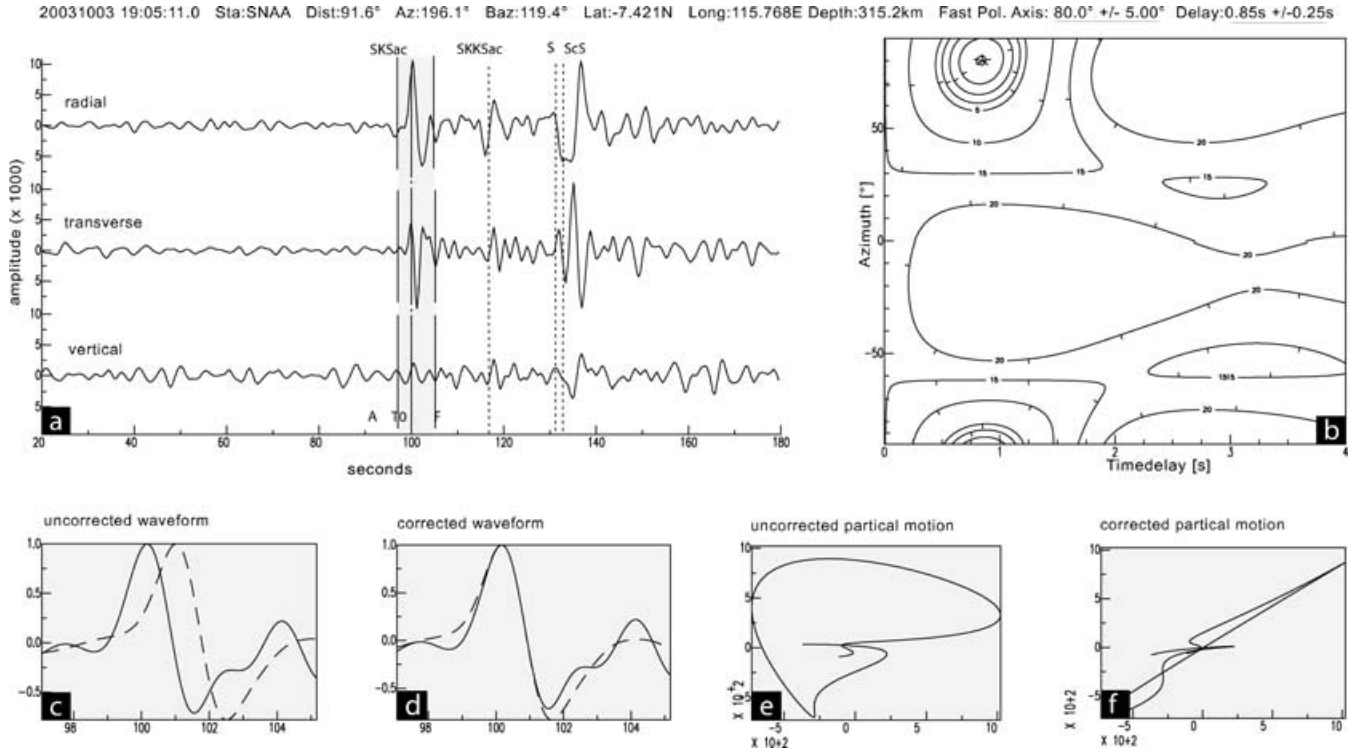

Figure 3. Example for a high quality measurement retrieved on station SNAA: (a) shows clear energy on the radial and transverse component. Energy is restricted within the horizontal plane; (b) shows the contour plot of energy on the transverse component as a function of the time delay and the polarization angle of the fast split shear wave; (c) before minimizing the transverse energy in order to reverse the splitting process the horizontal waveforms are separated and have similar shapes; (d) shows the waveforms after reversing. The waveform were shifted by the estimated time delay. This imitates a waveform traversing through an imaginary isotropic medium; (e) demonstrates the typical elliptical particle motion for a splitted shear phase and (f) shows a linear particle motion in the horizontal plane after applying the correction.

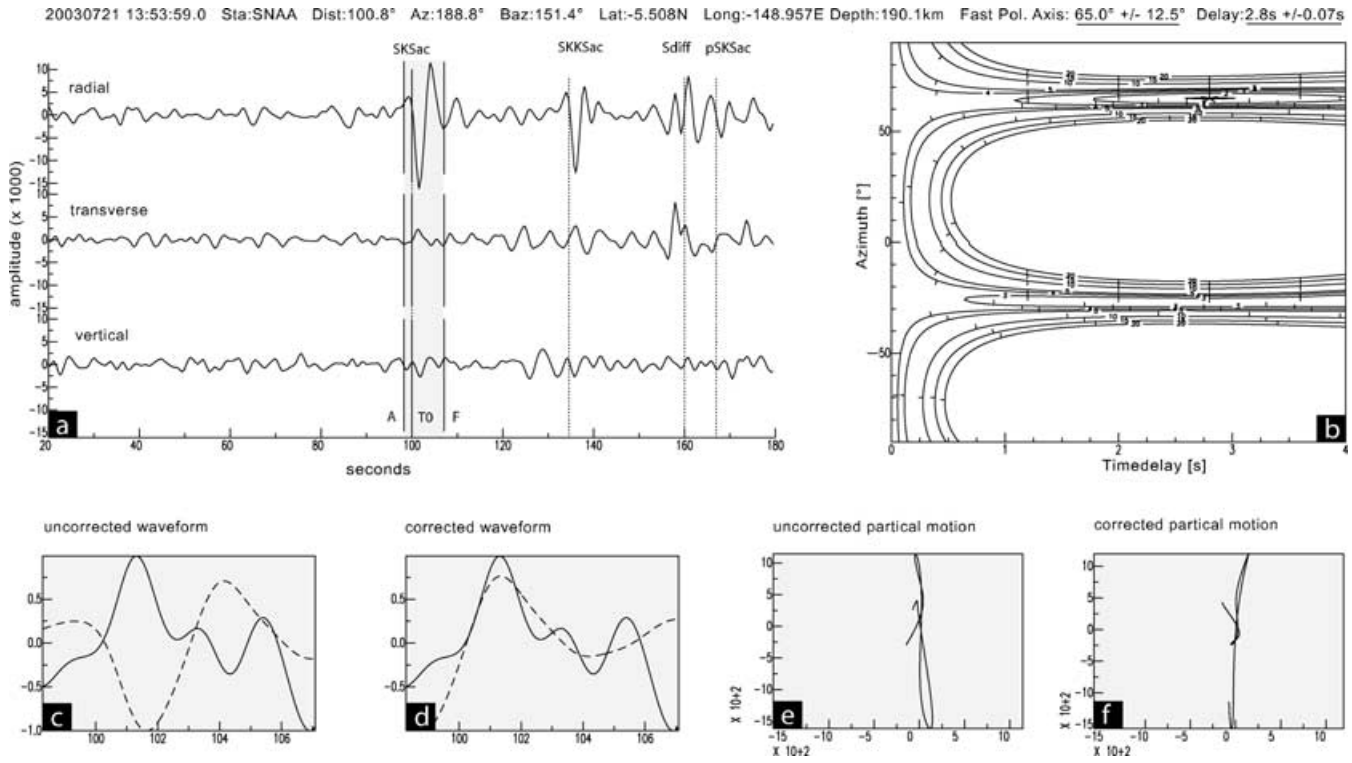

Figure 4. Example for a null measurement detected on station SNAA. Energy is restricted to the radial component as seen in (a). The elongated contour plot in (b) is one sign for a null measurement that pretend isotropy. The linear particle motion after minimizing the transverse energy is preserved. For a detail description of the individual inlay figures (a)–(f) see Fig. 3.

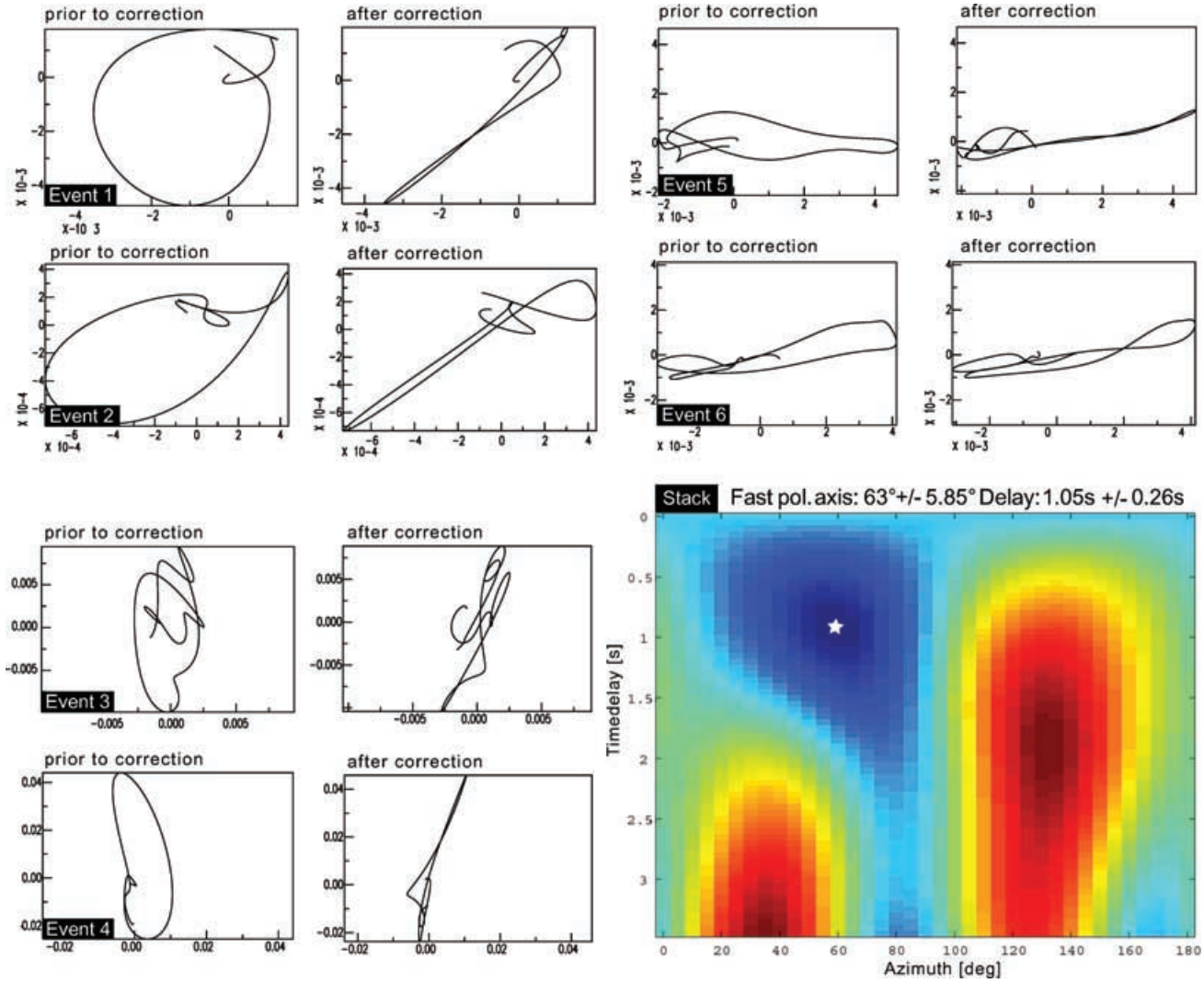

Figure 5. Particle motion prior to and after the correction of all data used into the stacking method after Wolfe & Silver (1998) for station KOH4. The final stacked splitting parameter pair is (63 ± 5.85°/1.03 ± 0.26 s). Individual values are provided as online supplementary data.

Within the HSZ, the Weigel nunatak is exposed. Here, the seismometer was deployed directly on solid rock during several south polar summer seasons and one winter period. A total of 13 sufficiently resolved splitted core shear phases were detected. Individual fast axis directions vary between 73° and 94° and overlap nearly within the 95 per cent confidence interval. Split times generally fall within the range of 0.72–1.38 s, although one measurement classified as fair yielded a higher time delay of 1.82 s. The multi-event stacking method yielded splitting parameter of (86 ± 5°/0.94 ± 0.25 s) (Table 1). We obtained nulls for shear phases with eastern, southern and western backazimuth (∼90°, ∼175° and ∼290°, respectively), consistent with simple single-layer anisotropy.

The observed splitting parameters for stations KOT1 and KOT4 at the western part of the HSZ were determined from single events with backazimuth of ∼100°, yielding splitting parameters of (34°/1.69 s) and (27°/1.50 s). For the stations temporarily deployed across the HSZ (KOH1–KOH6) we also applied the multi-event stacking method for at least five single events (Table 1 and Fig. 8). For station KOH6 we only obtained nulls, which is also consistent with simple single-layer anisotropy as the backazimuth of each event is parallel or perpendiculiar to the fast axis direction.

4.2 Results for NOVO, CDML

NOVO is situated close to the passive continental margin of the East Antarctic craton. A total of 23 sufficiently resolved core shear phases from teleseismic events with broad backazimuthal coverage were detected (Fig. 2). The estimated splitting parameter were not consistent with each other as predicted for a homogeneous single-layer and showed a $\pi/2$-periodicity.

We applied the waveform inversion method after Özalaybey & Savage (1994) to those shear phases with best SNR (Table 2). Including four phases, the inversion yielded splitting parameter of (64.3 ± 6.7°/0.68 ± 0.14 s) and (95.9 ± 7.3°/0.55 ± 0.21 s) for the upper and lower layer, respectively (Fig. 9). To reinforce the retrieved two-layer model, we applied the apparent splitting parameter modelling after Silver & Savage (1994). The theoretical splitting parameter were forward calculated for a two-layer model that yielded splitting parameter for each layer we retrieved from the waveform inversion technique. The estimated individual apparent splitting parameters fit these theoretical curve very well (Fig. 9). We remark that analysis of shear wave splitting at the coastal Neumayer station (Müller 2001) also yielded evidence for double-layer anisotropy

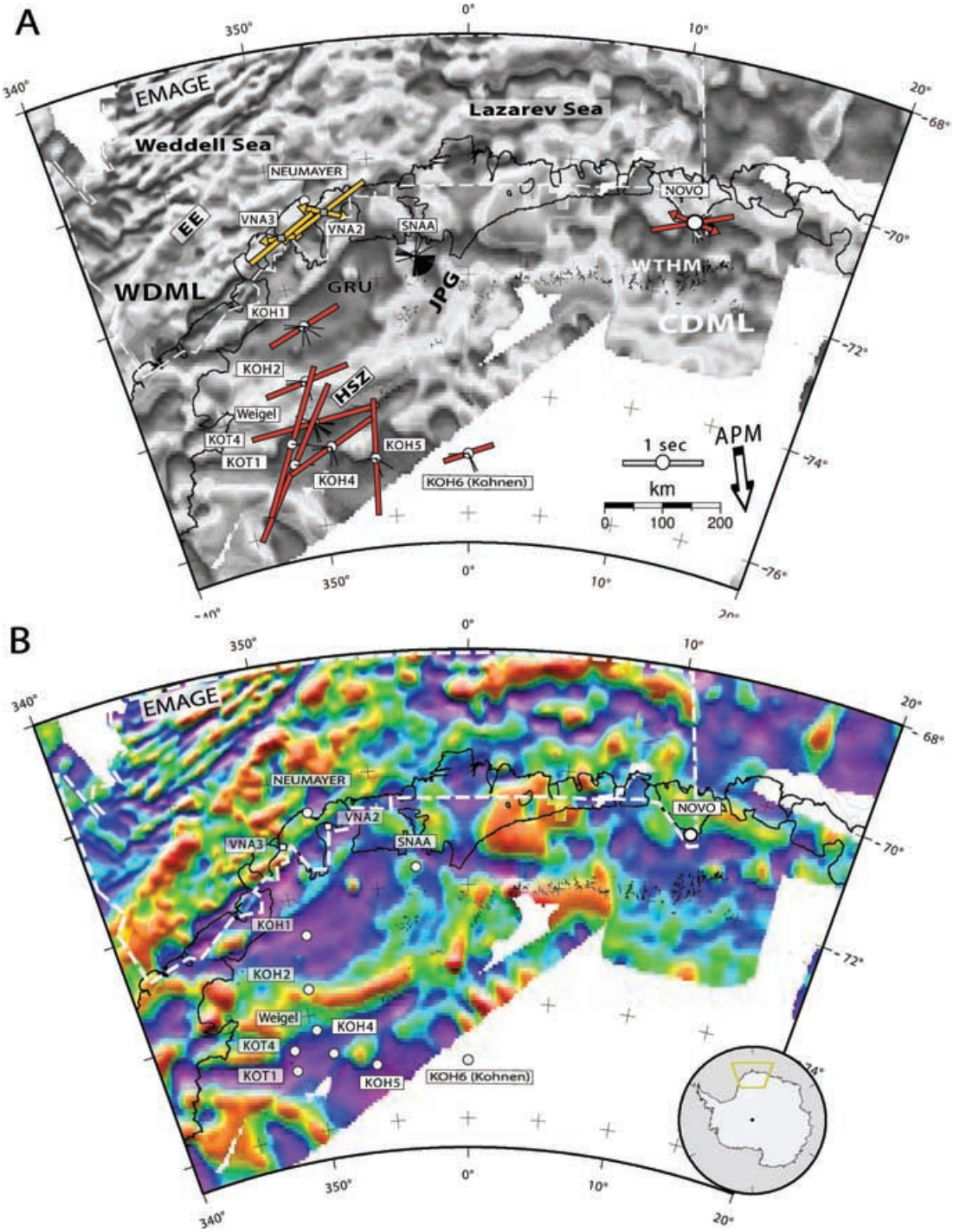

Figure 6. (A) Estimated splitting parameters plotted over grey scaled high resolution aeromagnetic anomaly grids of DML [EMAGE grid (Jokat *et al.* 2003) surrounded by a white dashed line and ADMAP grid (Golynsky *et al.* 2001)]. Thick red bars indicate fast axis θ and length is proportional to time delay δt. For coastal stations Novo and Neumayer (Müller 2001) models with two anisotropic layers are retrieved. Lower layers are signed with arrows. Thin black bars on the stations dot denote backazimuths of included phases. (B) Aeromagnetic anomalies in a coloured scale. Obviously, the fast axis of stations deployed across HSZ, Novo and Neumayer are aligned in a parallel manner with small-scaled geological features. Abbreviations are: EE, Explora Escarpment; JPG, Jutul-Penck-Graben; GRU, Grunehogna craton; CDML, Central Dronning Maud Land; WDML, Western Dronning Maud Land; WTHM, Wohlthat massif; APM, Absolute Plate Motion. Station names are listed in Table 1.

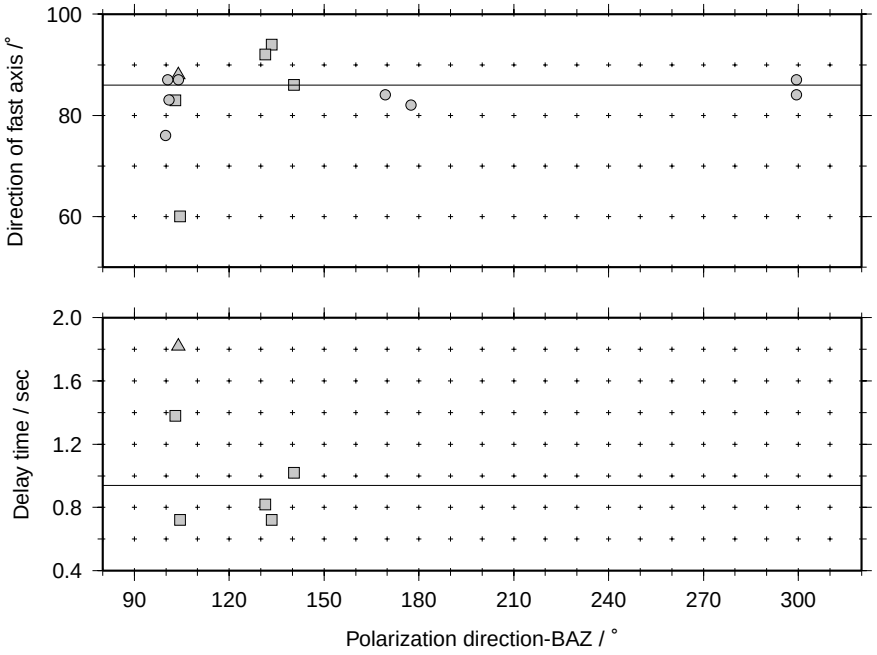

Figure 7. Splitting parameters derived from events for temporary deployed station at Weigel nunatak. Squares are measurements showing distinct anisotropy (good), triangles represent weaker but observable anisotropy (fair), circles denote nulls. Solid lines represent the stacked splitting parameter (86°/0.94 s).

with a similar difference (*ca*. 30°) between both fast directions of the two layers.

4.3 Results for Sanae IV (SNAA)

SNAA is located on the Archean to mid-Proteozoic aged Grunehogna craton, which is flanked at the eastern side by the Jutul-Penck-Graben, an old rift system completely covered by the Jutulstraumen glacier. It may conceal a buried lithospheric boundary between the Grunehogna craton and the mid-Protezoic to Cambrian Maudheim province (Groenewald *et al.* 1991). More than hundred phases of teleseismic events (Fig. 2 and online supplementary data) with hypocentral depth larger than 30 km, showing sharp onsets and steep incident angles, were taken into account and led to the most puzzling observation of shear wave splitting within the area of investigation. Neither a clear distribution nor a typical $\pi/2$-periodicity of the splitting parameter was found. The bulk of investigated phases show nulls over a broad range of backazimuth. For close backazimuthal segments, splitting parameters show strong variations. Isotropic and anisotropic measurements are close together and overlap in terms of the backazimuth (Fig. 10). Calculated individual error bars for fast axes are less than $\pm 9^\circ$, for time delays it yields values less than ± 0.4 s. Clear split phases are resolved at distinct backazimuth segments of 120°, 180° and 270° (Fig. 3 and two more examples provided as online supplementary data). We compared the theoretical backazimuth with the real one derived from a polarization examination of the *P* wave. They do not show a significant scatter and vary between $\pm 5 - 10^\circ$. Shear phases, generated by earthquakes in the Fiji Island Region with BAZ approximately 180° and with high SNR, show strong energy on its vertical component. This might not be expected for radially polarized shear phases traversing through the core (a data example is provided as online supplementary data). Focusing geometrical aspects, a dipping layer may generate such a vertical refracted phase. It may be related to a lateral heterogenity from a remnant geological structure or may serve as an indicator for the Himalayan-type indenter-escape tectonics model for the southern part of the late Neoproterozoic/early Palaeozoic East African-Antarctic orogen proposed by Jacobs & Thomas (2004). We exclude this measurements from further anisotropic discussions because a more complex model with strong lateral heterogenity is required.

5 INTERPRETATION AND DISCUSSION

The area of investigation is not active tectonically at present, and the Antarctic continent is moving slowly with respect to the whole-mantle reference frame, with an absolute plate velocity of 1.15 cm a^{-1} in a direction of 170° in DML (Gripp & Gordon 1990) (Fig. 1). Estimated fast axes for the stations considered here are poorly correlated with this direction of APM. It therefore, appears unlikely that anisotropy caused by viscous drag at the base of the lithosphere from modern plate motions is a suitable model for our results. Rather, our data are more consistent with the model of frozen-in anisotropy within the upper mantle due to VCD. Silver *et al.* (2004) reached a similar conclusion for southern Africa, the conjugant part of Antarctica during the existence of Gondwana.

5.1 Heimefront shear zone, WDML

We have compared the direction of observed fast axes with available high-resolution aeromagnetic anomaly grids EMAGE (Jokat *et al.* 2003) and ADMAP (Golynsky *et al.* 2001) (Fig. 6b). This comparison provides important insight into possible links between mantle anisotropy and crustal structure. The signature of GRU is detectable as a broad, featureless negative region close to the coast and as a linear short-wavelength magnetic anomaly inland. The magnetic signature of the juxtaposed Maudheim province is characterized by a linear belt of alternating bands of elongated magnetic highs and lows (Golynsky & Jacobs 2001).

The magnetic pattern represents the crustal contribution of the magnetic field, whereas the observable anisotropy is mainly

Table 2. Results of the two-layer inversion method of (Özalaybey & Savage 1994) for all station included in these study. Estimated splitting parameters are given with 95 per cent confidence limits; subscripts u and l refer to upper and lower layers, respectively. Line ALL denotes the sum of the individual events, whereas line Apparent for coastal station NOVO is the result of an apparent splitting modelling after (Silver & Savage 1994). Except for station NOVO, no evidence for a double-layer medium were found.

Event origin	Fast axis θ^u (°)	Time delay δt^u (s)	Fast axis θ^l (°)	Time delay δt^l (s)
NOVO				
2005 02 05 12:23:18	64.2 ± 6.6	0.69 ± 0.15	96.0 ± 7.4	0.59 ± 0.22
2005 03 02 10:42:12	53.8 ± 15.2	0.35 ± 0.24	84.5 ± 9.5	0.88 ± 0.18
2005 05 14 05:05:18	70.2 ± 15.9	1.06 ± 0.45	99.8 ± 10.3	1.32 ± 0.43
2005 10 11 15:05:39	61.1 ± 8.5	0.83 ± 0.60	84.8 ± 6.2	1.00 ± 0.90
ALL	64.3 ± 6.7	0.68 ± 0.24	95.9 ± 7.3	0.55 ± 0.21
Weigel nunatak				
2004 12 28 09:39:06	80.4 ± 12.8	0.44 ± 0.33	95.1 ± 5.3	1.21 ± 0.46
2005 01 21 17:54:34	91.3 ± 19.8	0.49 ± 0.45	120.4 ± 10.2	1.31 ± 0.52
2005 05 05 12:23:18	114.7 ± 8.6	1.18 ± 0.20	145.1 ± 5.6	1.18 ± 0.57
2005 03 02 10:42:12	55.9 ± 7.2	0.50 ± 0.13	114.2 ± 4.4	1.17 ± 0.13
KOH1				
2003 01 21 02:46:47	110.1 ± 10.2	0.86 ± 0.31	45.5 ± 10.2	1.23 ± 0.32
2003 01 04 05:15:03	10.7 ± 10.0	0.86 ± 0.29	55.2 ± 8.4	1.11 ± 0.19
2002 12 27 13:28:36	85.7 ± 16.9	0.87 ± 0.35	39.2 ± 16.5	1.30 ± 0.55
KOH2				
2003 01 21 02:46:47	80.8 ± 10.3	0.90 ± 0.41	99.6 ± 7.2	1.49 ± 1.86
2003 01 04 05:15:03	44.2 ± 8.3	1.56 ± 0.60	35.6 ± 7.9	1.54 ± 0.56
KOH4				
2003 01 21 02:46:47	84.9 ± 46.7	0.52 ± 0.90	40.7 ± 27.3	1.25 ± 0.94
2003 01 04 05:15:03	39.9 ± 12.6	1.20 ± 0.52	34.5 ± 19.1	0.85 ± 0.55
KOH5				
2002 12 30 04:49:08	147.2 ± 11.4	1.32 ± 0.33	116.6 ± 7.6	1.28 ± 0.54
KOT1				
2005 01 04 09:13:11	39.9 ± 9.1	1.04 ± 0.57	29.6 ± 8.5	1.22 ± 0.64
KOT4				
2004 12 31 01:04:51	29.6 ± 25.8	0.55 ± 1.23	29.9 ± 17.8	0.85 ± 1.23

generated by the upper mantle. The obtained fast directions are subparallel to, and appear to correlate with, the small-scale magnetic anomalies within western DML. We suggest, therefore, that vertical coherent deformation of the lithosphere led to LPO of mantle minerals. This implies that both crust and upper mantle were coherently deformed and strongly coupled during late Neoproterozoic/early Palaeozoic orogenic episodes.

The abrupt change in fast-axis direction around the HSZ is particularly notable. Such an abrupt change strongly suggests that the shear zone penetrates through the crust into the upper mantle, juxtaposing mantle lithosphere with distinct anisotropic fabrics. Similar observations of abrupt changes in anisotropic parameters have been found in the European landmass, and interpreted by Babuska & Plomerova (2006) to reflect preservation of fossil anisotropic fabric during the assembly of the continent. In the case of DML, the HSZ formed by the assembly of Rhodinia during the Grenvillian orogeny and thus may represent a fossil suture, now expressed as change in seismic anisotropy.

5.2 Novolazarevskaya (NOVO), CDML

Unlike stations farther inland, our data imply a two-layer anisotropic model for station NOVO. We note that the fast polarization axis of the upper layer is parallel to the orogenic strike of the nearby Wohlthat massif (Fig. 6) and, according to Damaske *et al.* (2005), subparallel to a nearby elongated magnetic anomaly. We therefore, interpret this alignment to reflect fossil anisotropy caused by late Neoproterozoic/early Palaeozoic orogenic events that produced the massif.

The inferred fast axis of the lower layer at NOVO is parallel to the continental margin. We remark that our model for NOVO is consistent with results by Müller (2001) for the German research base Neumayer/WDML (stations VNA2 and VNA3 in Fig. 6). In the case of Neumayer, the upper layer corresponds well to fast axes of the South African Kaapvaal craton after restoring the continents, whereas the lower layer fast axis is parallel to the continental margin. Müller (2001) interpreted the lower layer to have been created during early Gondwana rifting stages. This interpretation is compatiable with our results at station NOVO.

We suggest three potential interpretations for the parallel alignment of the fast axes of the lower layer and the continental margin.

First, within systems of strike-slip, or transcurrent deformation, fast polarization axis tends to be parallel to strike-slip movement (e.g. Moma rift, Vinnik *et al.* 1992). A strike-slip deformation stage due to reactivation of old fault zones before the final fragmentation of Gondwana, as discussed in Jokat *et al.* (2003), might have aligned

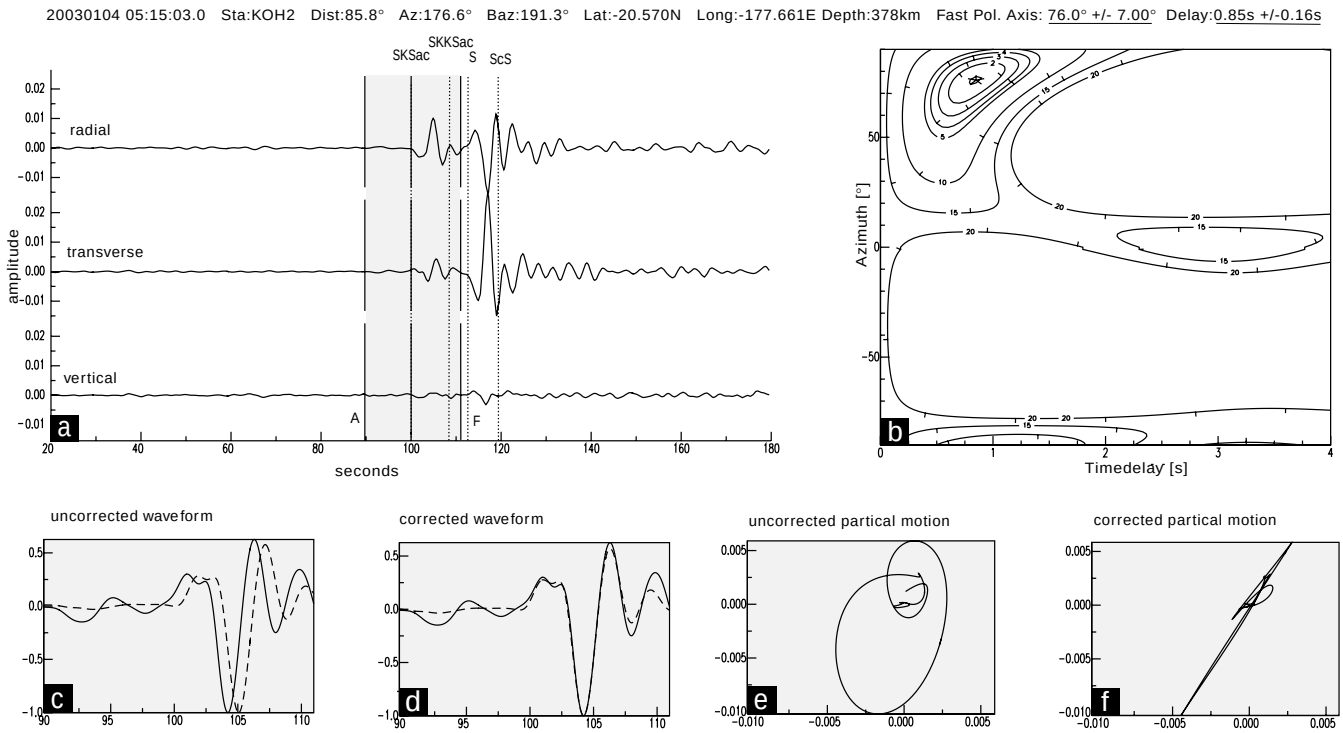

Figure 8. Example for a measurement with distinct anisotropy detected on temporary deployed station KOH2. The backazimuth of the event is 191° (Fiji Island Region). For a detail description of the individual inlay figures (a)–(f) see Fig. 3.

the minerals. Consequently, we support Gondwana break-up models for the region off NOVO taking strike-slip deformation into account before or during the rift phase. This is our preferred model.

Second interpretation suggests lateral flow along the rift at the time of opening of Lazarev Sea (the area off NOVO) during the most recent major event of Gondwana break-up. A parallel alignment of fast axes is also observed at stations deployed along the coast of East Greenland although no evidence for a double-layer anisotropic model is presented (Ucisik *et al.* 2005). On rift systems, orientation of fast axis is ambiguous, either orthogonal or parallel to extension direction, depending on a slow or fast spreading velocity, respectively (e.g. around East African Rift Gao *et al.* 1997). Jokat *et al.* (2003) inferred a rift system related to the opening of Lazarev Sea a slow full spreading rate of 3 cm yr^{-1} from aeromagnetic data. This study supports this item.

A third alternative involves a remnant slab of subducted material, either of oceanic or continental lithospheric origin associated with the late Neoproterozoic/early Palaeozoic Pan-African collision episode. Within continent–continent collisions one lithospheric block can be shifted over the other by cutting off the crust. This interpretation is rather speculative because no suture zone has yet been found due to ice coverage and the subsequent Jurassic continental break-up accompanied by tremendous heat might have destroyed any fabric especially on the base of the lithosphere.

5.3 Sanae IV (SNAA)

Due to the marked inconsistency of splitting measurements, one homogeneous anisotropic layer with vertical symmetry axis cannot explain our observations. We remark that M. Hoffmann (personal communication, 2006) calculated transverse receiver functions for SNAA and observed clear energy on the traces indicating intracrustal dipping layers and/or complex anisotropic behaviour. There are, however, many possible explanations for the complex splitting results, including:

First, near-vertical flow of mantle material (that is now frozen-in) during the break-up of Gondwana. In such a case the *a*-axis of olivine aligns vertically and anisotropy will not be detectable. This near-vertical flow could be related to a proposed mantle plume hypothesis with a plume-column underneath SNAA that subsequently led to the break-up of Gondwana (e.g. Jokat *et al.* 2003). According to fission-track analyses from Jacobs & Lisker (1999) it is proposed, that DML was covered by a thick layer of continental flood basalts.

Second interpretation suggests two or more anisotropic layers with different symmetry axes such that they cancel each other to make an effectively isotropic medium (Silver & Savage 1994). For a double-layer model in which the fast axes differ 90° from each other the anisotropic structures are not resolvable anymore. Double-layer models explain anisotropy sufficiently well for neighbouring seismological stations at Neumayer and NOVO.

A third alternative suggests complicated anisotropic properties that are not easily diagnosed with the simple method of shear wave splitting.

More measurements from closely spaced (temporary) seismic network will be required to investigate the pattern and geometry of anisotropic structures in more detail.

6 CONCLUSIONS

Investigations of shear wave splitting from core refracted *S* waves in DML, Antarctica, provides new insights into deeper geological structure and tectonic evolution of this region. Due to the harsh climate and inaccessibility of the terrain, long-term and dense seismic instrumentation is difficult to implement. On the other hand, due

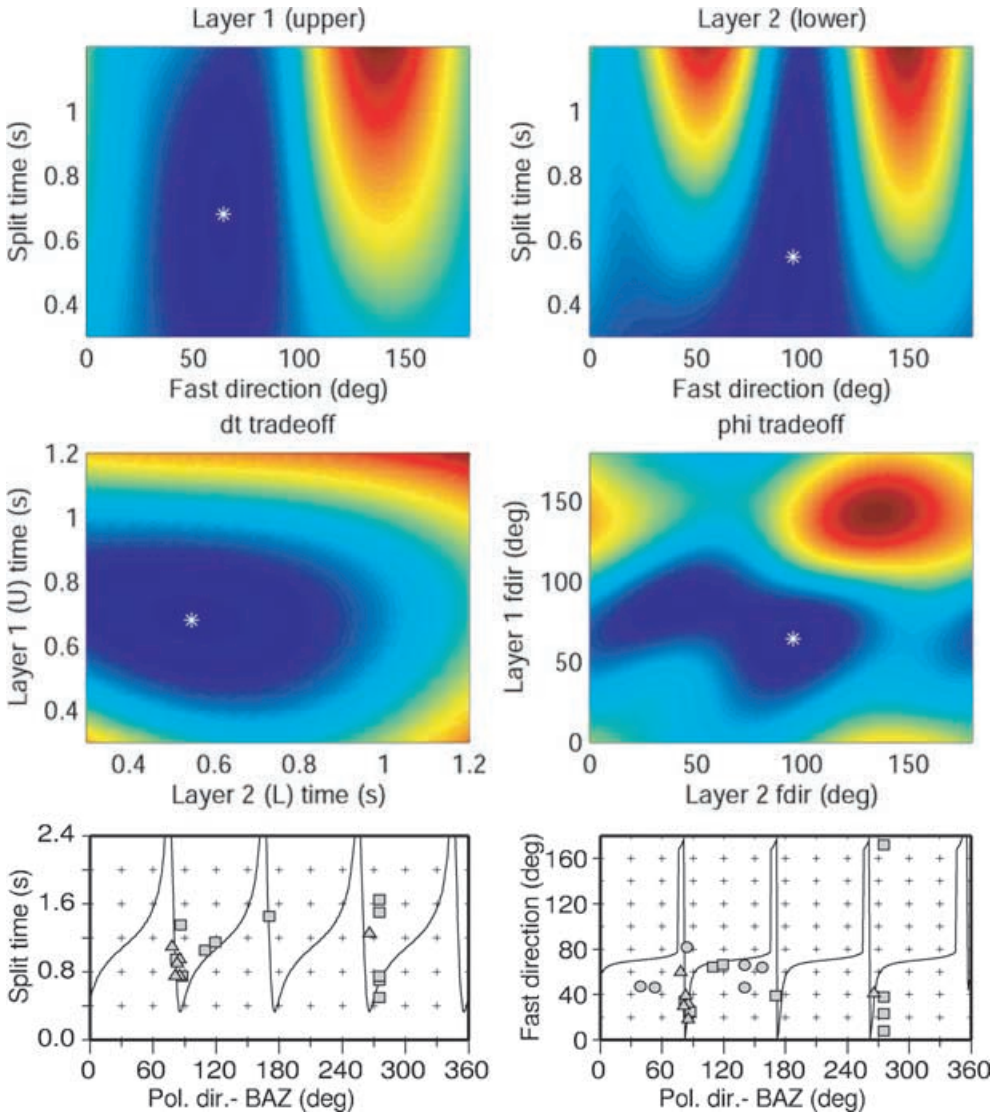

Figure 9. Two-layer model for station NOVO in CDML. Upper and middle plots represent the results we obtained from the waveform inversion method after Özalaybey & Savage (1994). As seen in the upper plot, splitting parameter (SP) of the shallower layer are (64.3 ± 6.7°/0.68 ± 0.24 s), of the lower (95.9 ± 7.3°/0.55 ± 0.21 s). Middle subplots demonstrate the tradeoffs between the SP pairs of both layers. Lower plots represent a comparison between single splitting measurements and a two-layer model, represented by solid computed using anisotropy values retrieved by waveform inversion. Squares are measurements with distinct anisotropy (good), triangles represent weaker but observable anisotropy (fair) and circles are nulls.

to the sparse knowledge about geological structures and tectonic evolution of Antarctica, every piece of evidence about tectonic fabrics is of great value for understanding lithospheric structure and development. In general, anisotropic structures are rather complex and reflect fossil fabrics of multiple tectonic events that formed the area of investigation. This area covers a region affected by major geological events ranging from structures created in the Archean of the East-Antarctic shield, Grenvillian and Pan-African orogenic events, and finally the Jurassic fragmentation of Gondwana. In detail, we conclude with following findings for our shear wave splitting analyses regarding mantle structures and geodynamic evolution of DML.

(i) Anisotropic features are probably not caused by asthenospheric flow, since present-day APM and anisotropic patterns are rather complex and too inconsistent across the network to be explained by simple asthenospheric flow.

(ii) In general, upper lithospheric anisotropic features follow the strike of major mountain belts. On a smaller scale, fast anisotropy directions follow the strike of magnetic anomalies. This implies that crustal anomalies correlate with fabrics in the deeper lithospheric mantle. Hence, it is reasonable to conclude that crust and mantle were strongly coupled in major orogenic episodes during assembly of the Antarctic continent.

(iii) The abrupt spatial variation in fast axes within HSZ suggests that the shear zone penetrate through the crust into the mantle, juxtaposing mantle layers with distinct tectonic histories. Hence, it enables us to support the hypothesis of the presence of a suture zone between the Archean Grunehogna craton and the Mesoproterozoic Maudheim province. This suture zone would cut the entire lithosphere.

(iv) At near-coastal stations there is strong evidence for double-layer seismic anisotropy. We interpret the lower anisotropic layers to reflect fossil fabrics created during first rifting stages of Gondwana

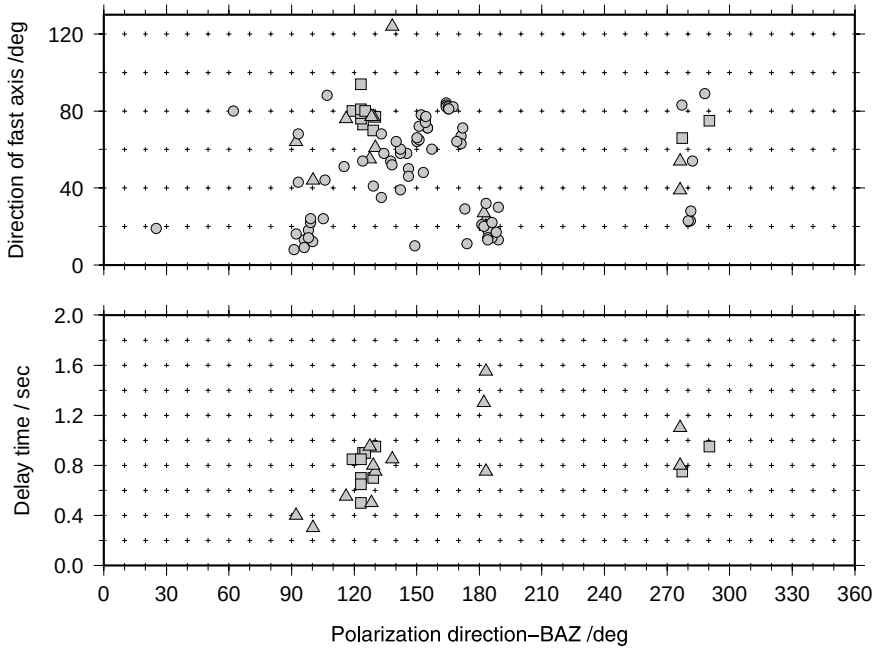

Figure 10. Splitting parameters derived from events deeper than 30 km for station SNAA. Note the strong variability of the splitting parameter. Measurements showing anisotropy and nulls are not consistent and overlap in close backazimuthal segments. Squares are measurements with distinct anisotropy (good), circles denote nulls. Triangles represent weaker but observable anisotropy (fair).

break-up, when deformation was dominated by strike-slip motion. Coastal stations like NOVO and results from the study of Müller (2001) for Neumayer station reveal exactly the same patterns for upper and lower layers, whereas stations further inland do not show evidence for a two-layer splitting.

(v) Inconsistent results regarding the azimuthal distribution of isotropic and anisotropic measurements were retrieved at SNAA. The observation of signal fractions on the vertical component suggest large scale lateral heterogeneous structures may be present. These complex lithospheric structures beneath SNAA, situated at the southeastern flank of the Grunehogna craton, may be due to a relict features associated with the transition from cratonic to Grenvillian/Pan-African orogeny. More data are needed to characterize this location.

These complex lithospheric evolutions affected by tectonic successions of continental collisions, lithospheric extension and fragmentation are strongly supported by the findings of our anisotropy investigations.

ACKNOWLEDGMENTS

This work would not have been possible without support of many scientists and technicians working in Antarctica and we gratefully wish to thank them all: Especially Mathias Hoffmann and Gertrud Waich for helping us managing major problems, Helgard Anschütz and Jens Köhler for doing some of the major seismological fieldwork, Matthias König for gmt and grid support, the colleagues of TU Dresden, the Russian and South African colleagues for their kind cooporation, Thomas Plenefisch, one anonymous reviewer and Editor Thorsten Becker for improving this manuscript. Partial support was given from the Natural Sciences and Engineering Research Council of Canada. Preparation of this work was supported by the Deutsche Forschungsgemeinschaft (DFG) through the VISA Project, funded under grants Di 473/17-1 and Jo 191/8-1.

REFERENCES

Artemieva, I.M. & Mooney, W.D., 2001. Thermal thickness and evolution of Precambrian lithosphere: a global study, *J. Geophys. Res. B: Solid Earth*, **106**(B8), 16 387–16 414.

Babuska, V. & Plomerova, J., 2006. European mantle lithosphere assembled from rigid microplates with inherited seismic anisotropy, *Phys. Earth Planet. Inter.*, **158**(2–4), 264–280.

Cox, K.G., 1992. Karoo igneous activity, and the early stages of the break-up of Gondwanaland, in *Magmatism and the Causes of Continental Break-up*, pp. 137–148, eds Storey, B.C., Alabaster, T., Pankhurst, R.J., Special Publication 68, Geological Society London.

Damaske, D., Marcinkowski, V. & Möller, H.-D., 2005. Aeromagnetic survey in central Dronning Maud Land, East Antarctica, during the 1995/1996 GeoMaud expedition: layout, execution, and data processing, in *Geologisches Jahrbuch, Reihe B, Heft 97*, pp. 53–83, Bundesanstalt für Geowissenschaften und Rohstoffe.

Eaton, D.W. & Jones, A.G., 2006. Tectonic fabric of the subcontinental lithosphere: evidence from seismic, magnetotelluric and mechanical anisotropy. Preface to special issue on Continental Lithospheric Anisotropy, *Phys. Earth Planet. Inter.*, **158,** 85–91.

Eaton, D.W., Jones, A.G. & Ferguson, I.J., 2004. Lithospheric anisotropy structures inferred from collocated teleseismic and magnetotelluric observations: great Slave Lake shear zone, northern Canada, *Geophys. Res. Lett.*, **31**(L19614), 1–4.

Fouch, M.J. & Rondenay, S., 2006. Seismic anisotropy beneath stable continental interiors, *Phys. Earth Planet. Inter.*, **158**(2–4), 292–320.

Gao, S. *et al.*, 1997. S K S splitting beneath continental rift zones, *J. Geophys. Res. B: Solid Earth*, **102**(B10), 22 781–22 797.

Golynsky, A. & Jacobs, J., 2001. Grenville-age versus Pan-African magnetic anomaly imprints in western Dronning Maud Land, East Antarctica, *J. Geol.*, **109**(1), 136–142.

Golynsky, A.V. et al., 2001. ADMAP—magnetic anomaly map of the Antarctic, 1:10000000 scale map, in *BAS (Misc.) 10*, eds Morris, P. & von Frese, R., British Antarctic Survey.

Gripp, A.E. & Gordon, R.G., 1990. Current plate velocities relative to the hotspots incorporating the NUVEL-1 global plate motion model, *Geophys. Res. Lett.*, **17**(8), 1109–1112.

Groenewald, P., Grantham, G. & Watkeys, M., 1991. Geological evidence for a Proterozoic to Mesozoic link between southeastern Africa and Dronning Maud Land, Antarctica, *J. Geol. Soc., Lond.,* **148,** 1115–1123.

Jacobs, J. & Lisker, F., 1999. Post permian tectono-thermal evolution of western Dronning Maud Land, East Antarctica: an apatite fission-track approach, *Antarctic Sci.,* **11**(4), 451–460.

Jacobs, J. & Thomas, R.J., 2004. Himalayan-type indenter-escape tectonics model for the southern part of the late Neoproterozoic-early Paleozoic East African-Antarctic orogen, *Geology,* **32**(8), 721–724.

Jacobs, J., Bauer, W. & Fanning, C.M., 2003. Late Neoproterozoic/early Palaeozoic events in central Dronning Maud Land and significance for the southern extension of the East African Orogen into East Antarctica, *Precambrian Res.,* **126**(1–2), 27–53.

Jokat, W., Böbel, T., König, M. & Meyer, U., 2003. Timing and geometry of early Gondwana break-up, *J. Geophys. Res. B: Solid Earth,* **108**(B9), 242B, doi:10.1029/2002JB001802

Montagner, J.P., 1994. Can seismology tell us anything about convection in the mantle?, *Rev. Geophys.,* **32**(2), 115–137.

Morelli, A. & Danesi, S., 2004. Seismological imaging of the Antarctic continental lithosphere: a review, *Global Planet. Change,* **42**(1–4), 155–165.

Müller, C., 2001. Upper mantle seismic anisotropy beneath Antarctica and the Scotia Sea region, *Geophys. J. Int.,* **147**(1), 105–122.

Özalaybey, S. & Savage, M.K., 1994. Double-layer anisotropy resolved from S phases, *Geophys. J. Int.,* **117,** 653–664.

Savage, M.K., Sheehan, A.F. & Lerner-Lam, A., 1996. Shear wave splitting across the Rocky Mountain Front, *Geophys. Res. Lett.,* **23**(17), 2267–2270.

Savage, M.S., 1999. Seismic anisotropy and mantle deformation: what have we learned from shear wave splitting?, *Rev. Geophys.,* **37**(1), 65–106.

Silver, P.G., 1996. Seismic anisotropy beneath the continents: probing the depths of geology, *Ann. Rev. Earth Planet. Sci.,* **24,** 385–432.

Silver, P.G. & Chan, W.W., 1991. Shear wave splitting and subcontinental mantle deformation, *J. Geophys. Res.,* **96,** 16 429-16 454.

Silver, P.G. & Savage, M.K., 1994. The interpretation of shear-wave splitting parameters in the presence of two anisotropic layers, *Geophys. J. Int.,* **119**(3), 949–963.

Silver, P.G., Fouch, M.J., Gao, S.S. & Schmitz, M., 2004. Seismic anisotropy, mantle fabric, and the magmatic evolution of Precambrian southern Africa, *S. Afric. J. Geol.,* **107**(1–2), 45–58.

Ucisik, N., Gudmundsson, O., Priestley, K. & Larsen, T.B., 2005. Seismic anisotropy beneath East Greenland revealed by shear wave splitting, *Geophys. Res. Lett.,* **32**(8), 1–4.

Vinnik, L.P., Makeyeva, L.I., Milev, A. & Usenko, A.Y., 1992. Global patterns of azimuthal anisotropy and deformations in the continental mantle, *Geophys. J. Int.,* **111**(3), 433–447.

Wolfe, C.J. & Silver, P.G., 1998. Seismic anisotropy of oceanic upper mantle: shear wave splitting methodologies and observations, *J. Geophys. Res. B: Solid Earth,* **103**(1), 749–771.